

Development of an Ingestible Fluid Wicking Gastric Electrical Stimulation Platform for
Hormone Modulation

By

James McRae

Submitted to the
Department of Mechanical Engineering
In Partial Fulfillment of the Requirements for the Degree of
Master of Science in Mechanical Engineering

At the

Massachusetts Institute of Technology

May 2022

© 2022 James McRae. All rights reserved.

The author hereby grants to MIT permission to reproduce and to distribute publicly paper and
electronic copies of this thesis document in whole or in part in any medium now known or
hereafter created.

Signature of Author: _____
Department of Mechanical Engineering
May 5th, 2022

Certified by: _____
Carlo Giovanni Traverso
Assistant Professor of Mechanical Engineering
Thesis Supervisor

Accepted by: _____
Nicolas Hadjiconstantinou
Professor of Mechanical Engineering
Chairman, Department Committee on Graduate Theses

Development of an Ingestible Fluid Wicking Gastric Electrical Stimulation Platform for Hormone Modulation

By

James McRae

Submitted to the Department of Mechanical Engineering on May 5th,
2022, in Partial Fulfillment of the Requirements for the Degree of

Master of Science in Mechanical Engineering

Abstract

Dysregulation of the gut-brain axis affects hundreds of millions of people annually, often resulting in motility, autoimmune, mood, and neurological disorders. Colloquially referred to as an “electroceutical,” electrical stimulation of the GI tract for modulation of this axis has been explored as a potential therapeutic for GI motility disorders. Thus far, these methods have utilized invasive implant procedures in order to stimulate the outer muscle layers of the stomach. The development of non-invasive stimulation approaches requires that these systems be in an ingestible form factor that instead stimulate the inner mucosal layer of the stomach. However, stimulation of the mucosal layer remains challenging due to gastric fluid that can disrupt targeted stimulation. In this work we first elucidate and establish the relationship between gastric electrical stimulation (GES) and the production of ghrelin, a hormone associated with hunger, in a pig model. Next, we translate this stimulation approach into a non-invasive capsule system that is then optimized through rapid iteration enabled by 3D printing and an *in vitro* system replicating the stomach’s mechanical and electrical properties. Finally, inspired by the fluid wicking skin of the *Moloch horridus*, we developed and integrated fluid wicking surface structures into the capsule that can displace fluid in order to mitigate the challenge it poses to targeted stimulation. The optimized capsule was administered *in vivo* in pigs and demonstrated the ability to modulate plasma ghrelin levels. The developments around the surface structure and properties to enable fluid displacement have broad ranging applications in low size, weight, and power (SWaP) ingestible mucoadhesive and fluid sampling systems.

Thesis Supervisor: Carlo Giovanni Traverso
Title: Assistant Professor of Mechanical Engineering

Acknowledgements

I would first and foremost like to thank my advisor Professor Giovanni Traverso of MIT's Department of Mechanical Engineering for allowing me the opportunity to pursue this work, providing unparalleled guidance and vision, always ensuring I had the resources I needed, fostering a supportive research environment, and helping me push the boundaries beyond what I thought I was capable of doing. I very much look forward to continuing on this path as I pursue my Ph.D. in his group.

Next, I would like to deeply thank Professor Khalil Ramadi of NYU for all of his close guidance, mentorship, and for being a pleasure to work alongside. His flexibility and availability to me given all of his responsibilities outside the group were absolutely vital in enabling me to push this project over the finish line, especially considering there were so many skills and techniques this project demanded that were brand new to me.

I would also like to thank all of those in the Traverso lab for their critical efforts and support in this project. Specifically, I would like to thank George Selsing for his incredible efforts on developing the electronics while also teaching me along the way. Additionally, huge thanks to Seokkee Min and Declan Gwynne for their support on the mechanical design, fabrication, and assembly. I have learned a great deal from all of these people and for that I am deeply appreciative. I would also like to thank all of the students and post-docs in the lab for fruitful and insightful conversation as well as camaraderie as I work through my graduate program. In particular I would like to thank Sanghyun Park as we have been side by side in the Mechanical Engineering graduate program, especially during our qualifying exam prep.

Next, I would also like to thank my close friend and colleague Bert Vandereydt of Professor Varanasi's lab for his friendship and for being an excellent and inspiring study partner in our successful preparation for the MechE Qualifying Exam.

Next, I would also like to acknowledge and thank the entirety of the animal team Keiko Ishida, Johannes Kuosmanen, Josh Jenkins, Weema Madani, Alison Hayward, and Niora Fabian for all of their incredible dedication and support with all of the in vivo work that was critical to the success of this work.

I would like to thank Professor Ken Kamrin of MIT's Department of Mechanical Engineering for all of his wonderful support and guidance surrounding the fluid mechanics aspects of this project. His insight and suggestions were very important to the development of this project.

I would like to thank Virginia E. Fulford for her support with the artwork in Figure 7 of this thesis.

Finally, I would like to thank all of the wonderful and inspiring undergraduate students both from here at MIT and outside of MIT I had the pleasure of mentoring for their eagerness to learn, contribute, and grow: Arnold Su, Brandon Rios, Maela Hickling, and Rafael Fernandes. I learned a great deal from working closely with all of you and look forward to keeping in touch in the future.

Contents

Table of Figures.....	6
1. Introduction.....	7
1.1 The Problem: Dysregulation of the Gut-Brain Axis	7
1.1.1 Gut-Brain Axis Overview and Impact of Dysregulation.....	7
1.1.2 Current Approaches to Treatment for Gastroparesis.....	7
1.2 Gastric Electrical Stimulation.....	8
1.2.1 GES for Gastroparesis.....	8
1.2.2 Ghrelin – The “Hunger Hormone”	9
2. In Vivo Validation of Ghrelin Modulation via Endoscopic Stimulation	9
2.1 Experimental Approach	10
2.1.1 Sedated Stimulation with Gold Probe	10
2.1.2 Stimulation in Vagotomized Animals	11
2.2 Hormone & Histology Analysis.....	11
3. Translating Endoscopic Stimulation Approach into Non-Invasive Device Platform	13
3.1 Core Challenges.....	13
3.1.1 Materials Optimization for Mucosal Contact	13
3.1.2 Form Factor Optimization for Fluid Management.....	13
3.2 Development of In Vitro Agarose Setup for Rapid Prototype Optimization	14
3.2.1 Material Optimization Leveraging Agarose Platform	16
3.2.2 Form Factor Optimization Leveraging Agarose Platform	17
3.3 Development of Bioinspired Fluid-Wicking Grooves	20
3.3.1 Fluid Channel Dimensions.....	21
3.3.2 Benchtop Evaluation of Optimized Capsules.....	25
4. In Vivo Demonstration	26
4.1 Hormone Modulation via E-stim Capsule	27
4.2 Device Safety	28
4.2.1 Localized Deployment	28
4.2.2 Passage Safety	29
5. Conclusion	31
5.1 Discussion.....	31
5.2 Future Work	33

Bibliography	34
Appendices	38
Device Design Details	38
Device Assembly Procedure	39

Table of Figures

Figure 1. Depiction and Images of In Vivo Endoscopic Gold Probe Experiment.....	10
Figure 2. Plasma ghrelin concentration against time for various stimulation parameters (A-D). Plasma hormone concentrations for various other hormones (GLP-1, Gastrin, VIP) at various pulse width stimulation parameters (E-G). Plasma ghrelin concentration comparing stimulation, sham, and vagotomized stimulation studies (H). H&E stained histology samples (I-L). Ghrelin antibody stained histology samples (M-P).....	12
Figure 3. Diagram and Depiction of Agarose Setup.....	15
Figure 4. Comparison of Stimulation Signal between Agarose Phantom and Ex Vivo Stomach Tissue	15
Figure 5. Depiction of Various Electrodes and Contact Resistance Data.....	16
Figure 6. Panel of Form Factor Designs and Down-Selection Process	19
Figure 7. Depiction of Thorny Lizard and Groove Dimensional Constraints. The author acknowledges Ginny for her contributions to the artwork. [35].....	22
Figure 8. Summary Panels of Benchtop Plasma Treatment Testing (Planar Samples + Capsules)	23
Figure 9. Depiction of Planar Groove Designs, Fabricated Samples, and Impedance Data.....	24
Figure 10. Ex Vivo Evaluation of Optimized Capsule	25
Figure 11. Time-lapsed Depiction of Fluid Wicking Capsule with Blue Dye.....	26
Figure 12. Depiction of Optimized Capsule In Vivo Administration and Plasma Hormone Levels	27
Figure 13. Depiction of Localized Deployment System Assembly and In Vivo Deployment....	28
Figure 14. Administration, x-ray evaluation, post-passage collection, and violin distribution chart of passage studies.....	29
Figure 15. Histology Samples from Various GIT Sections Following Device Passage.....	30

1. Introduction

1.1 The Problem: Dysregulation of the Gut-Brain Axis

Dysregulation of the gut-brain axis is associated with disorders that affect millions of people annually. Better understanding this complex network will aid in improving approaches to treating many of these disorders.

1.1.1 Gut-Brain Axis Overview and Impact of Dysregulation

The gut-brain axis is a complicated bi-directional network between the GI tract and the brain that consists of various nerve branches, hormonal pathways, and more. [1], [2] However, there are two main communication pathways that this system can be broken down into. [1] First, is the enteric nervous system (ENS) which is typically referred to as the “second brain” in that it regulates all GI function, and can continue to do so even when severed from the central nervous system. [2] The second communication pathway is through the circulatory system where hormones and other molecules that get secreted in the gut can diffuse into the circulatory system and get carried to the brain where they can then bind with the appropriate receptors.

Dysregulation of the gut-brain axis is associated with many disorders either directly, where dysregulation is known to cause the disorder, or indirectly where dysregulation is observed in tandem with the disorder. These disorders can range from motility, autoimmune, and neurological and ultimately affect 100s of millions of people annually. [3]–[8] Elucidation of specific mechanisms of disorder and dysregulation would open up significant opportunities for more targeted therapies. In addition, it opens up opportunities for novel therapies, such as electroceuticals. [9] Electroceuticals have the advantage of greater spatio-temporal resolution given that specific nerves can be targeted and stimulated to induce an effect in seconds or minutes.

Thus far, electrical stimulation approaches for gastroparesis have been most widely explored both in academic literature and clinically. Gastroparesis is a motility disorder characterized by delayed gastric emptying that is often accompanied by symptoms such as chronic nausea and vomiting.

1.1.2 Current Approaches to Treatment for Gastroparesis

The following sections will focus mainly on gastroparesis as it is the main disorder that has had significant academic and industry efforts invested in addressing it although its etiology is still unknown. [3] The main treatments for gastroparesis depend heavily on the severity of symptoms,

but commonly involve dietary modifications or the use of antiemetic (nausea and vomiting) or prokinetic medications (acid reflux). [10] More recently, hormonal therapies such as motilin and ghrelin, as well as neuromodulators have also been explored as they increase gastric emptying. [11] Additionally, gastric electrical stimulation (GES) has been evaluated as a potential treatment where in place of medications, electrical stimulation is used as a treatment method.

1.2 Gastric Electrical Stimulation

GES as the acronym suggests is the use of electrical stimulation in the gastric environment as a treatment approach, namely for gastroparesis, but with the potential for many other disorders. In literature, GES has been explored for gastroparesis, obesity, and more. [12]–[15] This purpose of the electrical stimulation is to either induce muscle contractions or activate or inhibit specific nerves that may play a role in certain disorders. [16], [17]

1.2.1 GES for Gastroparesis

The original intent of GES for gastroparesis was to use the electrical stimulation to induce muscle contractions that would aid in the digestion of food and reduce gastric emptying time, effectively behaving as a pacemaker for the stomach. Medtronic commercially developed a system aimed at achieving this, known as the Enterra™. [18], [19] This is a surgically implanted device where the external electronics and power supply are tethered to two electrodes which get inserted and sutured into the outside of the stomach in the serosal muscle layer. However, what is observed over and over again is that the electrical stimulation does not reduce gastric emptying time (the parameter that defines gastroparesis) but it does reduce the symptoms associated with gastroparesis such as nausea and vomiting. [20]–[24] Given the observed reduction in symptoms, this device is still considered a treatment option for gastroparesis.

1.2.2 Ghrelin – The “Hunger Hormone”

While GES does not reduce gastric emptying time but does reduce nausea and vomiting symptoms, it is of interest to identify what is mediating the stimulation’s effect on symptoms. What has been demonstrated thus far is that GES using Enterra™ parameters has induced increases in plasma ghrelin levels. [25] Ghrelin is an orexigenic hormone (appetite stimulating) that is produced in the enteroendocrine cells that line the GI tract. Ghrelin levels tend to increase in anticipation of a meal and subside after feeding. Additionally, ghrelin agonists, or molecules that bind to ghrelin receptors, are being explored as potential treatments for chronic nausea and vomiting. [26] Taken in full, these findings indicate that GES via Enterra™ parameters increases plasma ghrelin levels and that ghrelin-like molecules may have the ability to reduce nausea and vomiting, thus indicating that ghrelin is likely what is mediating the clinical findings that GES does not reduce gastroparesis but does reduce its symptoms.

Establishing the mediating link between the electrical stimulation and the biological response is critical in identifying and developing potential therapeutic approaches using electrical stimulation, colloquially referred to as ‘electroceuticals.’ [9] This provides an appropriate signal that can be experimentally monitored and modulated during GES studies to help inform specific approaches and mechanisms.

2. In Vivo Validation of Ghrelin Modulation via Endoscopic Stimulation

Thus far, commercially available gastric electrical stimulation systems are surgically implanted and there have been no demonstrations of stimulation done via the gastric mucosa in literature. [19], [25] In order to develop a non-invasive ingestible platform for gastric electrical stimulation, the ability to modulate ghrelin via mucosal stimulation from within the stomach must be demonstrated. Additionally, the exact mechanism of ghrelin modulation in response to gastric electrical stimulation is not well-understood. To better understand potential mechanisms of ghrelin modulation, gastric electrical stimulation was done bilaterally vagotomized pigs to help elucidate the role of the vagus nerve and neuronal stimulation.

2.1 Experimental Approach

2.1.1 Sedated Stimulation with Gold Probe

Endoscopic gastric electrical stimulation was carried in out sedated pigs (30-75kg Yorkshire Swine) used a bipolar gold probe commonly used for electrocautery, as portrayed in Figure 1. [28] Blood samples were taken at various time points (-20, -10, 0, 5, 10, 15, 20, 30, 40, 60, and 90 minutes) and centrifuged to extract plasma samples that were stored in the -80 °C fridge for subsequent hormone analysis via ELISA. The endoscope allows for controlled spatial placement and orientation of the gold probe electrodes to ensure reliable contact for delivery of stimulation. Additionally, the endoscope enables removal of excess gastric fluid to prevent parasitic losses and the ability to insufflate the stomach for proper visualization.

Various stimulation parameters (stimulation time, pulse amplitude, and pulse width) were evaluated in vivo to determine the optimal stimulation parameters. Stimulation times of 5, 20, and 60 minutes were evaluated. Pulse amplitudes of 0.5 and 5 mA were evaluated. Finally, pulse widths of 0.3 ms and 3 ms were evaluated.

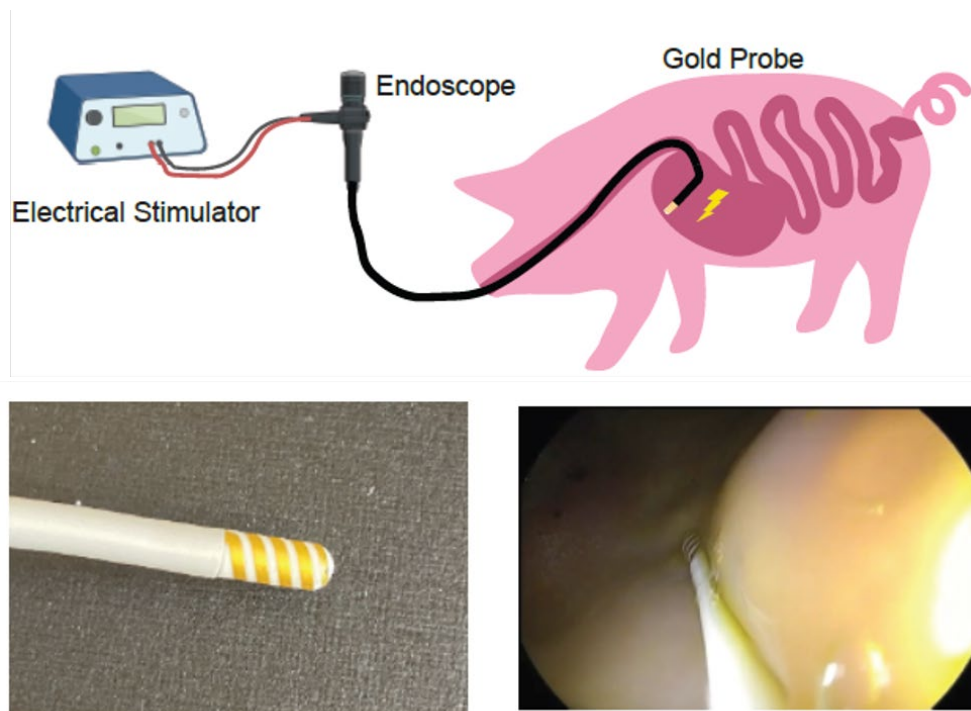


Figure 1. Depiction and Images of In Vivo Endoscopic Gold Probe Experiment

2.1.2 Stimulation in Vagotomized Animals

The vagus nerve is a critical nerve that plays a significant role in gut-brain communication and controls many autonomic functions such as breathing, heart rate, blood pressure, and GI motility. [29] To elucidate its potential role in ghrelin modulation via GES, stimulation studies as described previously were performed on vagotomized animals (fully severed vagus nerve).

2.2 Hormone & Histology Analysis

Blood was collected from animals via venous catheter into EDTA tubes (5mL/tube). For ghrelin analysis, EDTA tubes were prefilled with 4-(hydroxymercuri)benzoic acid sodium (10mM, 300uL). Blood was centrifuged at 3000rpm for 10minutes. Plasma was carefully removed and distributed into 500mL aliquots. 10% 1N HCl was added to each vial prior to storage at -80C. Blood collected for other hormone analysis was prefilled with pefabloc, a cocktail of protease inhibitors (Roche). Hormone analysis was conducted using a number of enzyme-linked immunosorbent assays (ELISA): Ghrelin Acylated Porcine ELISA (BioVendor R&D, Asheville, NC), GLP-1 Porcine ELISA (MyBioSource), Gastrin Porcine ELISA (Biomatik, Wilmington, DE), VIP Porcine ELISA (LSBio, Seattle, WA).

In addition to plasma hormone analysis, histology samples were taken at mucosal regions near the site of stimulation and far away from the site of stimulation. These samples were then stained with H&E to compare tissue morphology between the two locations and evaluate if stimulation has a damaging effect on tissue. Additionally, histology samples were stained with ghrelin antibodies to identify the location of ghrelin within the tissue at both locations, shown as the brown spots in Figure 2. It was determined that there were no noticeable differences between locations by Dr. Bronson of the Koch Institute Histology Core. Additionally, no discernable differences were qualitatively observed in the ghrelin antibody staining.

For sufficient ghrelin modulation, it was determined that 0.5 mA pulse amplitude with 0.3 ms pulse width at 14 Hz for 20 minutes was sufficient to observe significant ghrelin modulation, as demonstrated in panels A-H in Figure 2. Panels E-G indicated plasma concentrations for various other hormones GLP-1, gastrin, and VIP of which all but VIP show some level of modulation with various pulse width stimulation parameters. Interestingly, a decrease in plasma ghrelin was observed in vagotomized animals, shown in panel H.

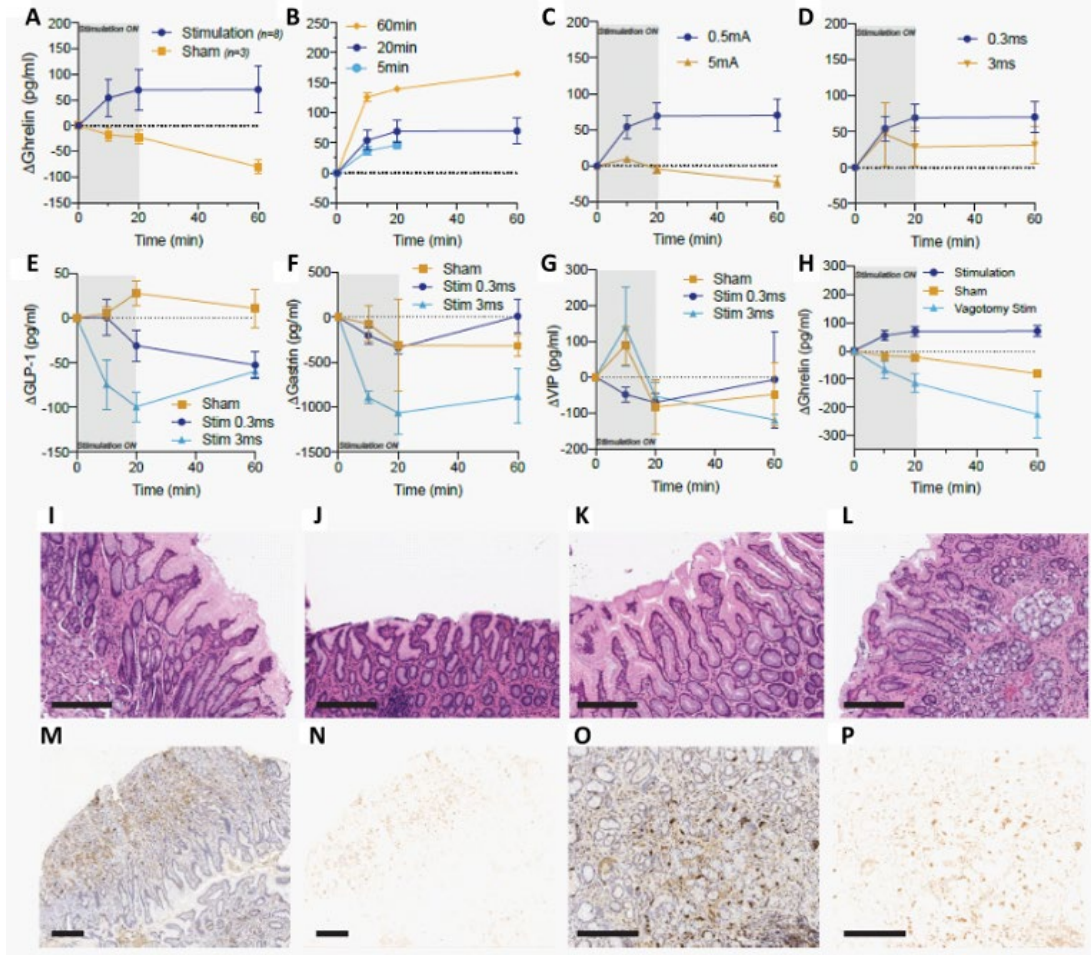


Figure 2. Plasma ghrelin concentration against time for various stimulation parameters (A-D). Plasma hormone concentrations for various other hormones (GLP-1, Gastrin, VIP) at various pulse width stimulation parameters (E-G). Plasma ghrelin concentration comparing stimulation, sham, and vagotomized stimulation studies (H). H&E stained histology samples (I-L). Ghrelin antibody stained histology samples (M-P).

3. Translating Endoscopic Stimulation Approach into Non-Invasive Device Platform

3.1 Core Challenges

There are two core challenges to the development on a non-invasive, ingestible stimulation capsule. First, the capsule materials, in particular the electrode materials, must be optimized in order to promote the lowest impedance interface between the electrodes and the mucosa. The larger the impedance, the larger the power budget will be for the system which directly effects size considerations of the platform. Second, the capsule form factor must be designed with the intent of facilitating reliable interactions between the electrodes and the mucosa given the dynamic and often fluid-immersed environment within the stomach.

3.1.1 Materials Optimization for Mucosal Contact

Materials optimization, in particular the electrode material, is of critical importance to the development on a non-invasive ingestible stimulation platform. The boundary conditions on maximum overall capsule dimensions are well defined by clinical data around systems leveraging the OROS capsule dimensions (9x15 mm). [30] This capsule system resembles that of a 000 capsule (9.5x26 mm) which is the largest size of standard capsule available. Within ingestible electronic systems, a significant portion of this volume is typically occupied by the batteries. Within this stimulation capsule platform, the vast majority of our power budget is allocated to the generation and delivery of the electrical stimulation between the two concentric-wound electrodes. Therefore, the impedance of the interface between the electrodes and the mucosal surface will critically inform the power draw of the system and thus the impedance of this interface will need to be optimized in order to accommodate the electronics and power supply within the volume boundary constraints.

3.1.2 Form Factor Optimization for Fluid Management

Ensuring reliable contact between the electrodes and the stomach mucosa is of critical importance to ensure the stimulation is able to be reliably delivered to the appropriate location. Gastric fluid within the stomach poses the risk of shorting the electrical stimulation elsewhere in the stomach, thus reducing or potentially preventing the stimulation from being delivered to the appropriate location along the mucosa. In summary, gastric fluid within the stomach poses a significant risk to ensuring reliable electrical stimulation via an ingestible stimulation platform.

Therefore, form factor modifications must be considered in order to manage the gastric fluid in order to ensure reliable contact. Without addressing this challenge, an ingestible stimulation platform will be plagued by inability to properly deliver stimulation due to the dynamic and complex stomach environment.

3.2 Development of In Vitro Agarose Setup for Rapid Prototype Optimization

Given the vast parameter space to evaluate when optimizing this ingestible stimulation capsule (materials, form factor, etc.), it is not feasible to move directly into in vivo studies. Therefore, a benchtop model that is able to replicate the stomach mucosa is of great importance to enable high throughput prototype evaluation and iteration to hasten the optimization process before moving to large animal models. Critically, this benchtop system must properly capture the mechanical and electrical properties of stomach tissue such that it can accurately simulate the interactions the stimulation capsule would have in in vivo conditions.

Agarose gels are commonly used as tissue phantoms for various different applications. [31], [32] In this system, a 100x100x5 mm agarose sheet was cast into a silicone mold which a stimulation device and an oscilloscope can be connected to in order to deliver current from the stimulation system through the agarose tissue phantom. This signal is then measured by the oscilloscope. This setup is highlighted in Figure 3.

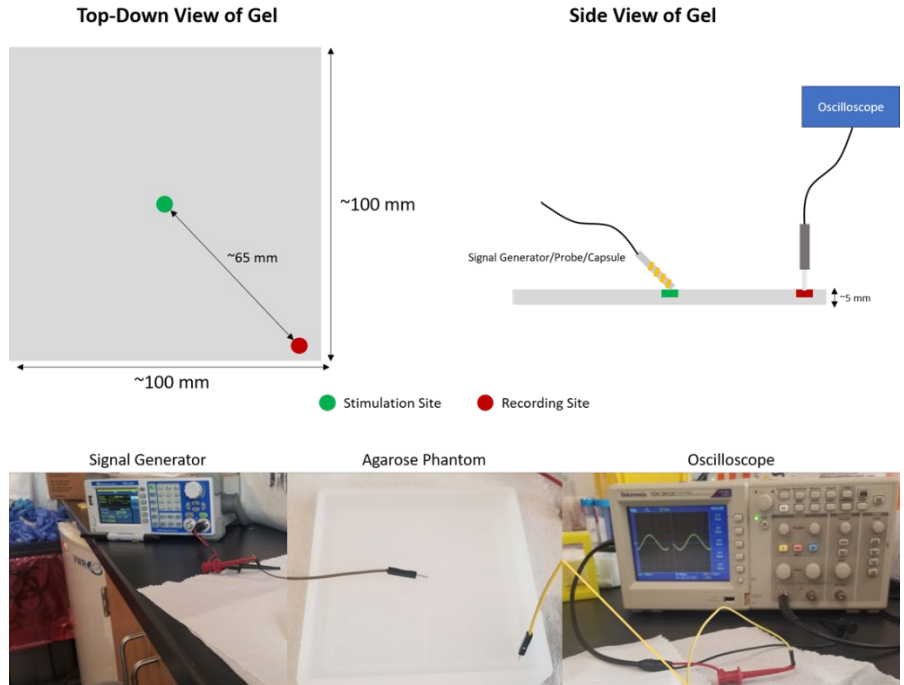


Figure 3. Diagram and Depiction of Agarose Setup

The mechanical properties of agarose can be tuned via the composition of the agarose in the mixture in order to closely match that of stomach tissue. [33], [34] This work utilized an agarose composition of 2 percent by weight in a phosphate-buffered saline (PBS) solution. The electrolytic PBS allowed for a more accurate representation of tissue impedance and was experimentally determined to be on the order of 100s of Ohms, as shown in Figure 4.

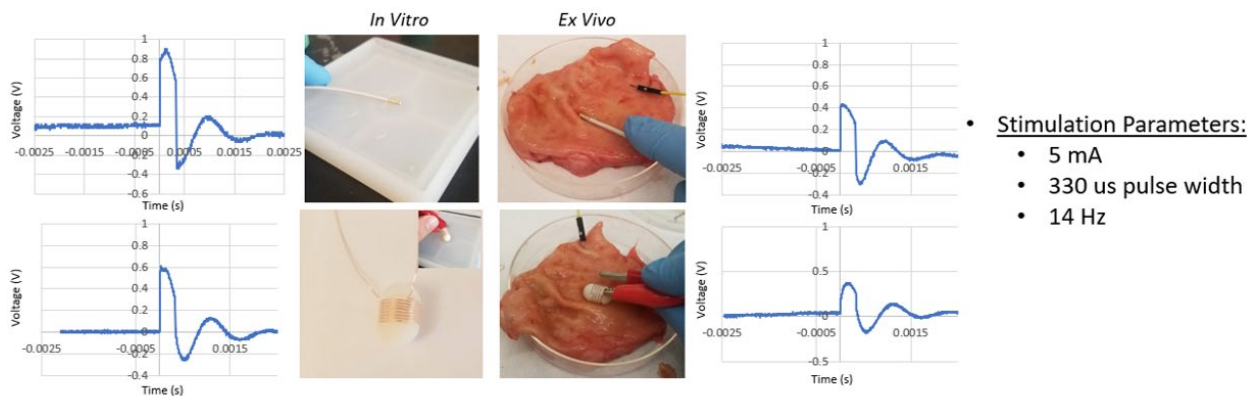


Figure 4. Comparison of Stimulation Signal between Agarose Phantom and Ex Vivo Stomach Tissue

Now with the mechanical and electrical properties resembling that of stomach tissue, this system can be used to rapidly evaluate a broad range of systems in order to optimize the delivery of stimulation to the agarose phantom. Additionally, the flat sheet of agarose resembles a worst-case scenario with respect to total surface area contact between the electrodes and tissue, thus it is expected that in actual scenarios the system will require an even lesser voltage due solely to the effect of surface area contact on resistance.

3.2.1 Material Optimization Leveraging Agarose Platform

To optimize the electrode material, four potential materials were evaluated: copper wire, 14K gold wire, gold-coated nitinol wire, and gold ribbon. These electrodes were incorporated into a capsule system, as represented on the left in Figure 5, and were then placed on the in vitro agarose tissue phantom and the resulting signal was measured with an oscilloscope. In addition to lowest measured resistance, it is important to account for the cost of the material and the ease of integration into prototypes. Ideally a balance between all three of these factors will be necessary to determine the optimal material that has the lowest resistance that is not prohibitively expensive and can be easily integrated into capsules to avoid fabrication, assembly, and reliability bottlenecks when rapidly evaluating the stimulation capsule. The resulting voltage signals as measured by the oscilloscope using the agarose phantom are highlighted in the graph in Figure 5 where we see the resistance from highest to lowest being copper, 14K gold, gold-coated nitinol, and finally gold ribbon.

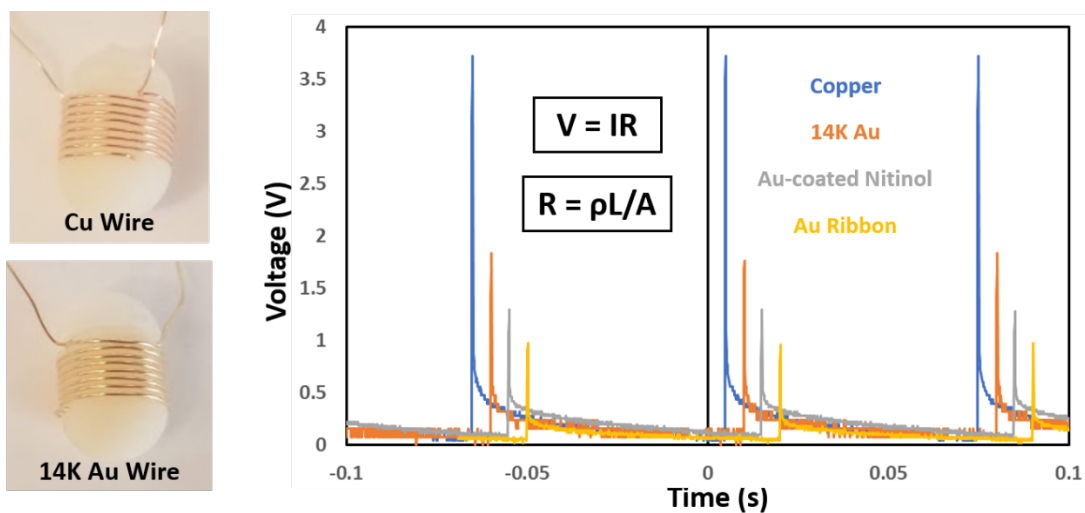


Figure 5. Depiction of Various Electrodes and Contact Resistance Data

Observations for all of these electrode materials is compiled into Table 1 below. The main observations for copper are that it has high resistance and poor stability in caustic environments like the stomach. The 14K gold have a relatively low resistance and is corrosion-resistant and not prohibitively expensive. The gold-coated nitinol had an even lower resistance, but given the superelastic properties and special manufacturing techniques it is challenging to reliably integrate and is fairly expensive. Finally, the gold ribbon faired best with respect to resistance. However, it is challenging to concentrically wind flat ribbons around a capsule, the pure gold itself is prohibitively expensive, and the flat form factor prevents the electrode from properly contacting the mucosa compared to a wire form factor that can be pressed into the mucosa. Thus, the 14K gold wire was selected as the optimal electrode material.

Table 1. Compilation of Observations from Electrode Optimization Experiments

Electrode	Observation
Copper	<ul style="list-style-type: none"> • High Impedance • Poor chemical resistance
14K Gold	<ul style="list-style-type: none"> • Low impedance • Resistant to corrosion
Gold-coated Nitinol	<ul style="list-style-type: none"> • Integration challenges/stiff • Expensive
Pure Gold Ribbon	<ul style="list-style-type: none"> • Very expensive • Integration challenges/fragile

3.2.2 Form Factor Optimization Leveraging Agarose Platform

Next, the form factor of the ingestible system has significant impact on its effectiveness and thus must be taken into consideration in the design process. First, the high-level shape of the system must be chosen such that the device can safely pass through the GI tract and can enable repeatable orientation and contact with the stomach tissue, as shown in Figure 6. As a starting point, the OROS-shaped capsule provides a good baseline. The OROS system is a 9x15 mm capsule that is a solid dosage form for osmotic drug release. There are dozens of FDA-approved

devices with these general dimensions, and clinical data has shown a retention rate of roughly 1 in every 30 million administrations, indicating excellent safety. [30] Additionally, one can consider spherical or tabular systems. A spherical system would ensure uniform contact dynamics between the entire capsule and its surrounding. However, given the form factor and volume requirement for the electronics and power supply that the capsule will house, spherical systems do not allow for facile integration and would hinder the rapid iteration. Similarly, one can consider tabular based systems that would behave similarly to a coin in that they are only mechanically stable when laying on one of its two faces. Similarly, given the form factor of the off-the-shelf electronics and batteries, integration into a system with this form factor becomes significantly challenging. Therefore, with regards to high-level device shape, a capsule based system was selected.

Next, the electrode surface area plays a critical role in determining the resistance of the contact between the electrodes and the tissue. Ultimately, a higher resistance for a given constant current pulse profile will translate to a higher power budget. Given the tight volume constraints on ingestible devices for safety of both administration and passage, it is critical to minimize the power budget such that unnecessary volume is not used up by the batteries and so that overall capsule dimensions can remain within the boundaries of what is clinically safe. Given the simple resistance equation:

$$R = \frac{\rho * L}{A} \quad (1)$$

It is evident that resistance and cross-sectional area, or in this case the surface area in contact with the mucosa, have an inverse relationship. Thus, maximizing the electrode surface area will reduce the overall interfacial resistance. Starting from the OROS capsule, the electrode surface area can be increased by 1) decreasing the electrode wire pitch and 2) increasing the length of the capsule within the bounds of what is still considered safe, in this case a 000 capsule which is the largest available pill size with dimensions of 9.5x26 mm. The obvious choice here is the capsule with the largest possible surface area which would be a tight-pitch 000 capsule, as highlighted in Figure 6.

Finally, the surface patterning of the capsule must be modified to facilitate and enable optimal contact between the surface electrodes and the gastric environment. Given the fluid present in the gastric environment, it is important to consider how the surface can be leveraged to enable

repeatable and reliable orientation between the capsule and the mucosa. Potential surface patterns to achieve this goal are displayed in Figure 6.

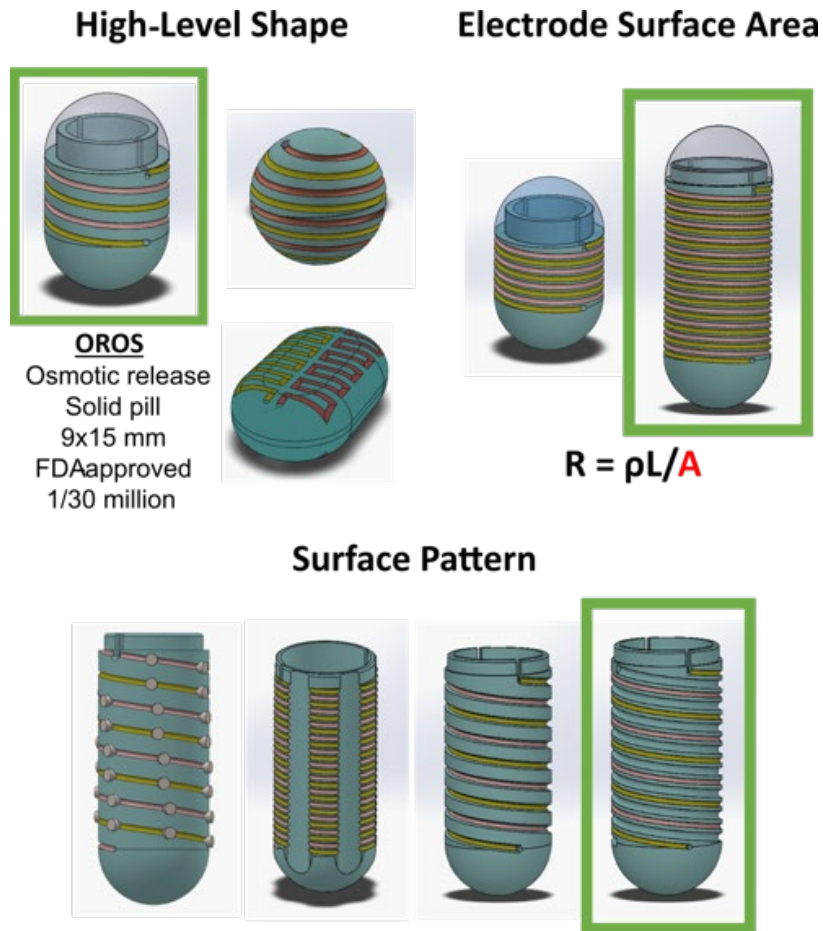


Figure 6. Panel of Form Factor Designs and Down-Selection Process

One can first consider radially-extending posts that would protrude into the mucosa as extensions of the electrodes themselves. This would enable the electrodes to effectively be pressed into the mucosa and occluded from any gastric fluid because it would be surrounded by stomach tissue. However, integrating radially-extending electrode posts poses two challenges. First, is a safety challenge relating to overall device size. Extending posts from the surface will exceed the 000 capsule dimensions and pose a risk to scratching the mucosa due to their relatively high aspect ratio. Additionally, fabricating and reliably integrating many electrode posts reliably dramatically complicates fabrication and increases assembly time, ultimately hindering the high throughput workflow that will facilitate the identification of a suitable solution. Future work can consider form

factors with radially-extending electrode posts as there are still potential benefits to this approach if the safety and fabrication challenges can be addressed.

Next, one can consider integrating grooved channels into the capsule surface in order to channel gastric fluid away from the surface where the electrode is contacting the mucosa. The analogy here is that of a tire treads which are used to channel fluid away in order to facilitate optimal contact between the tire material and the road. Next, the orientation of the channels is of great importance. Channels running vertically along the capsule length will not effectively channel gastric fluid away from the side of the capsule in contact with the mucosa, it will only pool up fluid in this region and hinder contact. Therefore, channels that run in the azimuthal direction will be needed such that fluid collected at the electrode-tissue interface can be pulled up around the capsule to the other side that is not in contact with the tissue.

When considering this orientation, there are two potential ways to integrate these grooves. The first would incorporate deep groove recessions with the electrodes placed at the bottom, and the second would reduce the total number of electrode wraps by alternating each electrode wrap with a fluid-wicking groove. Ultimately the latter option is the only feasible option, as in the first option, the fluid has the potential to fully occlude the electrode from the mucosa if the mucosa is unable to fully press into the groove. Therefore, it is optimal to sacrifice reduction in total electrode surface area for the ability to wick fluid away from the electrode interface. This may prove to be necessary in cases where, without the grooves, the increased electrode surface area would have a null effect because of the capsule's inability to properly contact the mucosa. The final form factor decision was to develop a 000 capsule with alternation electrodes and fluid-wicking grooves at minimum pitch.

3.3 Development of Bioinspired Fluid-Wicking Grooves

The surface fluid-wicking behavior takes inspiration from the Australian Thorny Lizard, as highlighted in Figure 7. This lizard leverages its surface textured skin to passively manage fluid in order to maintain hydration in an arid environment without having to actively expend time and energy to seek out water. Our pill aims to adapt this passive fluid management behavior in order to manage the gastric environment where there is typically an excess of fluid that, when delivering

electrical stimulation, can behave as a source of parasitic loss that can drain the electrical current elsewhere from the desired mucosal stimulation site.

Incorporating passive fluid management functionality is critical to the device volume and power constraints. Otherwise, active fluid management systems would require more power and volume dedicated to the electronic systems that enable the fluid management. Being able to integrate sufficient fluid management in a passive system enables significant capability within the small volume and power budget of the overall system.

3.3.1 Fluid Channel Dimensions

First, the dimensions of the fluid channel must be optimized to ensure that the wicking ability of the capsule is maximized. To do this, we will model the grooves as vertical capillary channels and compare the wicking volume capability. We can consider various groove cross-sectional shapes, but in this work, we will only consider the two most simple to fabricate, those being a rectangular and spherical shape as shown in Figure 7. When considering these as vertical capillary channels, the equation is a simple force balance between the capillary force on the fluid and the static fluid pressure times the groove cross-sectional area, resulting basically in the weight of the fluid. These can be re-arranged to solve directly for the fluid wicking height, as shown in the equations in Figure 7.

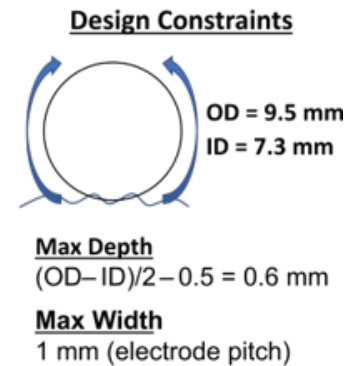
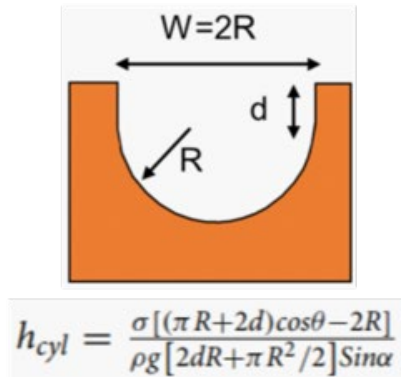
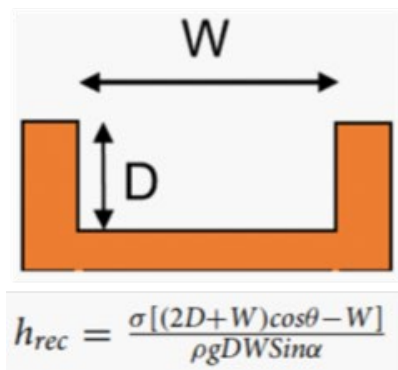
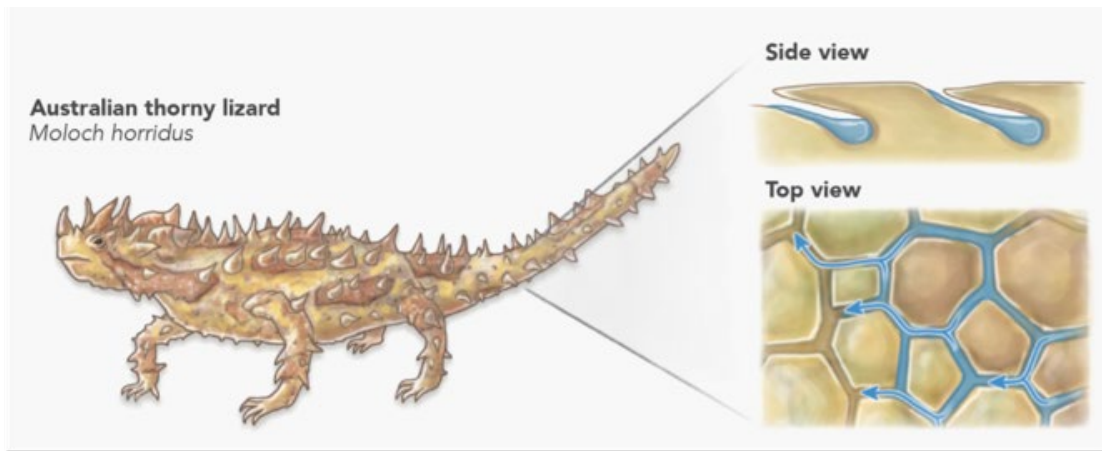


Figure 7. Depiction of Thorny Lizard and Groove Dimensional Constraints. The author acknowledges Virginia E. Fulford for her artwork. [35]

The parameters that are available to tune for optimizing the fluid wicking height, and thus ultimately the fluid wicking volume, are the groove dimensions (D, W, R, d) and the contact angle between the fluid and the groove surface given that the contact angle can be modulated by modulating the surface properties of the grooves. The other parameters such as fluid density, gravitational constant, fluid surface tension, and the channel angle are not parameters that can be modified as they are fixed parameters in this system.

First the channel dimensions must be determined. In order to do so, boundary conditions must be placed on these dimensions in order to provide a framework for the optimization space. Given that the capsule without grooves has a wall thickness of 1.1 mm and the minimum wall thickness that will provide mechanical robustness is 0.5 mm, the max groove depth is 0.6 mm. Regarding groove width, the maximum width a groove can be when alternating between electrodes

and grooves without significantly reducing the overall electrode surface area is 1 mm. These dimensions inform the boundary conditions on the fluid wicking grooves.

These dimensions can then be plugged directly into the capillary rise equations. However, the only missing value is then the contact angle between the fluid and the groove surface. To characterize and optimize this, a series of O₂ plasma treatments were performed on planar samples of the same material the grooves are made of. The O₂ plasma treatment modifies the non-polar polymeric surface molecules into hydroxyl groups, imparting a higher surface energy that is much more strongly attracted to water molecules. All of this work is highlighted in Figure 8. Without plasma treatment, the contact angle between water and the planar sample was approximately 54 degrees. With sequentially increasing plasma treatments at 1 minute and 50 W, 5 minutes and 50 W, and 5 minutes and 100 W a continual decrease in contact angle is observed. Given the lowest contact angle at 5 minutes and 100 W plasma treatment, this contact angle value is used in the capillary rise equations.

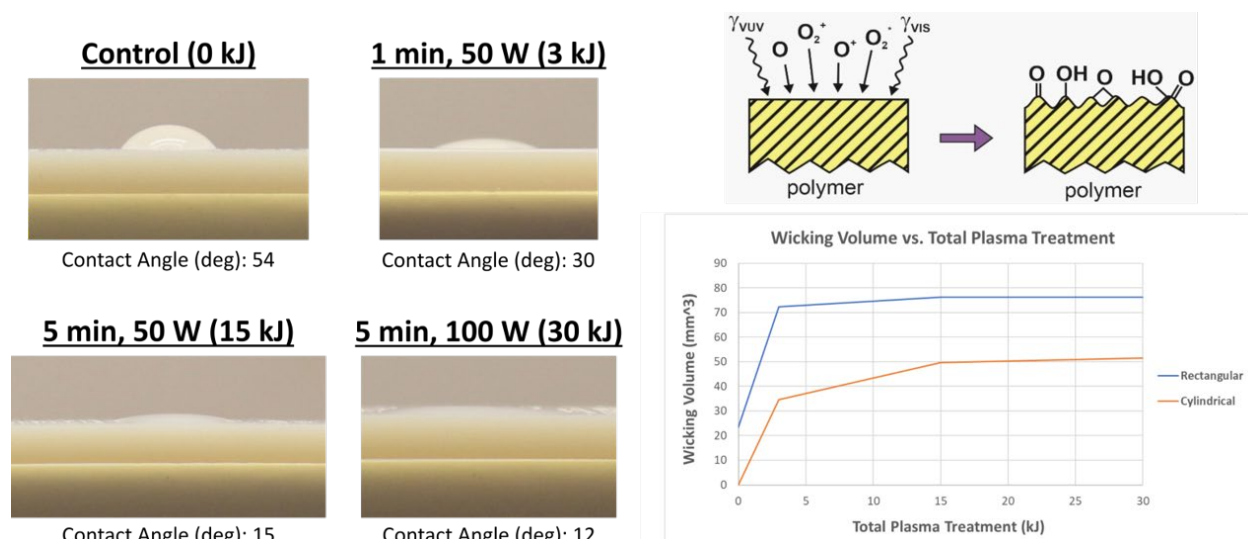


Figure 8. Summary Panels of Benchtop Plasma Treatment Testing (Planar Samples + Capsules)

Now with the groove dimensions of 1x0.6 mm and the contact angles evaluated, the fluid wicking heights were calculated for both square and circular groove cross-sections as a function of total plasma treatment and converted to wicking volumes by multiplying by cross-sectional area, as shown in the graph in the bottom right of Figure 8. At all plasma treatments, the rectangular

grooves have a greater fluid wicking capability and the total volume wicked starts to taper off as you get to higher and higher plasma treatments. From these results, it was determined that rectangular grooves are optimal for the fluid wicking capsule surface.

Next, in order to experimentally determine optimal rectangular groove dimensions, planar samples were fabricated via additive manufacturing that contained groove dimensions of various depths and widths, as shown in Figure 9. Groove width ranged from 0.1 mm to 2 mm and groove depth ranged from 0.5 mm to 2 mm.

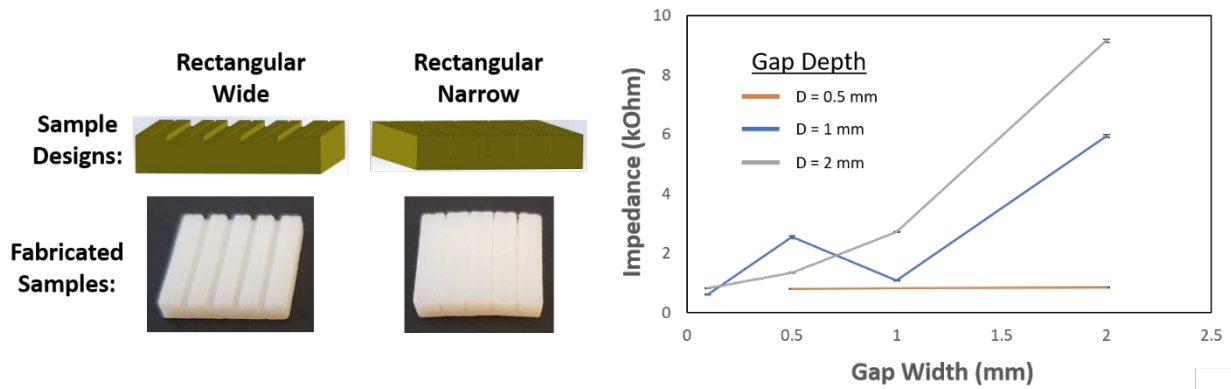


Figure 9. Depiction of Planar Groove Designs, Fabricated Samples, and Impedance Data

These results determined that increasing the gap width increases the contact impedance only as the gap depth is increased. One potential explanation for this phenomenon is that at shallow gap depths, capillary action can still happen as you increased gap width because the cross-sectional area of the groove is still fairly small, and thus the weight needed the channel needs to wick is relatively small. However, as the cross-sectional area increases (as it does significantly with increasing gap depth) the weight of the fluid becomes more significant and thus the fluid may more significantly impede the contact between the electrode and the mucosa. Based on this data, optimal groove dimensions would align either at a gap depth of 0.5 mm or at a gap depth of 1 or 2 mm but a gap width of 0.1 mm. Given that we would like to optimize total wicking volume, the obvious choice is the groove with the largest cross-sectional area which would be the 1 mm wide by 0.5 mm deep groove. Interestingly, this aligns well with our theoretical findings with the capillary rise equations.

3.3.2 Benchtop Evaluation of Optimized Capsules

Now that the groove dimensions have been optimized and experimentally validated, it is now time to incorporate these groove dimensions in an actual capsule platform to evaluate performance on the benchtop before finally moving to in vivo administration. Ex vivo evaluation of the contact impedance as well as micro-CT images validating fluid-channel formation are displayed in Figure 10. Here, the CAD with the optimized grooves incorporated as well as a SEM image are provided to show the design and fabrication of these capsule systems. These optimized capsules were then wound with electrodes and connected to an impedance analyzer. A small volume of real gastric fluid was dispensed onto ex vivo pig stomach tissue and the capsule was placed onto the region with the fluid. This was done with two grooved capsules, one with treatment and one without. As shown in Figure 10, the grooved capsule with plasma treatment shows a significant reduction in impedance compared to the non-treated capsule.

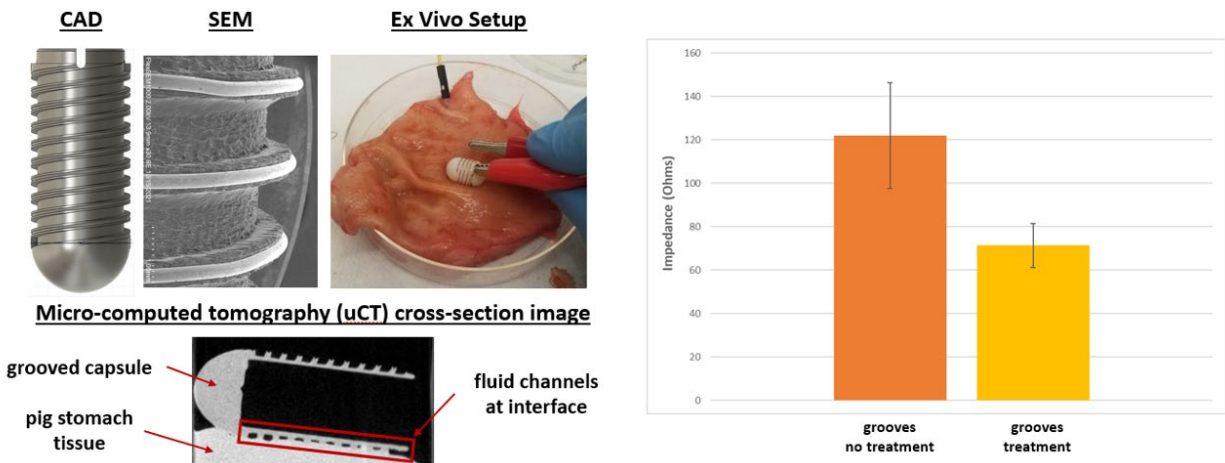


Figure 10. Ex Vivo Evaluation of Optimized Capsule

In addition, to validate that fluid-wicking channels are in fact created when the capsule contacts stomach tissue, a capsule was placed on a small portion of ex vivo stomach tissue and a micro-CT scan was taken. A cross-sectional image of the micro-CT scan shows that there are indeed channels created where the grooves are in the capsule. In addition, this shows that the electrode regions are pressed into the mucosa given the high aspect ratio of the groove walls where the electrodes sit inside.

Next, a benchtop visual demonstration of fluid wicking was performed, as shown in Figure 11. Here, three capsules were fabricated. The first capsule has the optimized groove dimensions but did not undergo plasma treatment. The second capsule has a smooth outer surface but did undergo plasma treatment. The final capsule has the optimized grooves and did undergo plasma treatment. Each capsule had 200 μ L of methylene blue solution dispensed directly underneath it. The first capsule showed no fluid wicking behavior at all. The second capsule showed slight attraction of the fluid, but was unable to actually wick up the bulk fluid due to the lack of volume and capillary forces to do so. The third capsule showed immediate fluid wicking behavior with the grooves rapidly managing all of the dispensed fluid in less than one minute. Beyond this time point, the capsule continued to channel the fluid down the spiral grooves until the fluid was fully wicked by the capsule, whereas the first two capsules still were sitting in a puddle of methylene blue solution. This demonstration confirms the necessity of both the mechanical groove dimensions as well as the plasma treated surface to more readily wick the liquid.

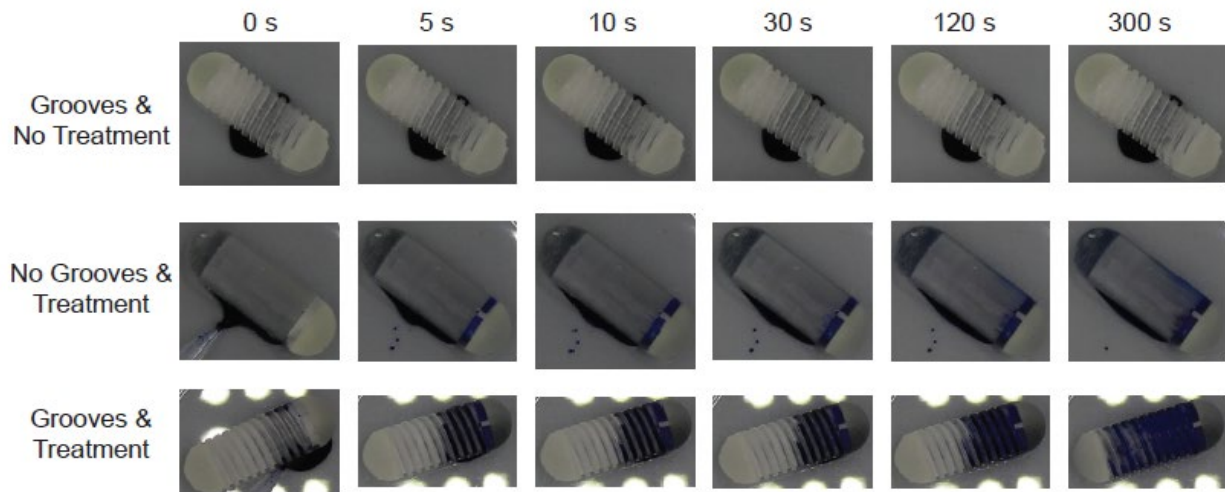


Figure 11. Time-lapsed Depiction of Fluid Wicking Capsule with Blue Dye

4. In Vivo Demonstration

There were four main criteria that needed to be evaluated with the optimized capsule. The first criteria is that the capsule must demonstrate the ability to modulate hormones, as was demonstrated with the endoscopic gold probe studies previously described. Second, the capsule must be able to be locally deployed to the region of interest, given the fact that pre-mature

stimulation or fluid wicking is not desired. Third, the capsule must be able to safely pass through the GI tract and remain intact. Fourth and final, the capsule must not cause damage and inflammation to the GI tract. These four criteria are discussed in greater detail in the following sub-sections.

4.1 Hormone Modulation via E-stim Capsule

In order to evaluate the hormone modulation capability of the capsule, full prototypes were fabricated, assembled, and delivered to sedated swine. See the “Device Assembly Procedure” Appendix for more details on prototype fabrication and assembly. Once the capsules were validated before administration, the capsule was delivered to a sedated pig via an over tube, as shown in Figure 12. The capsule was then located in the stomach to ensure it was intact and was properly contacting the mucosa.

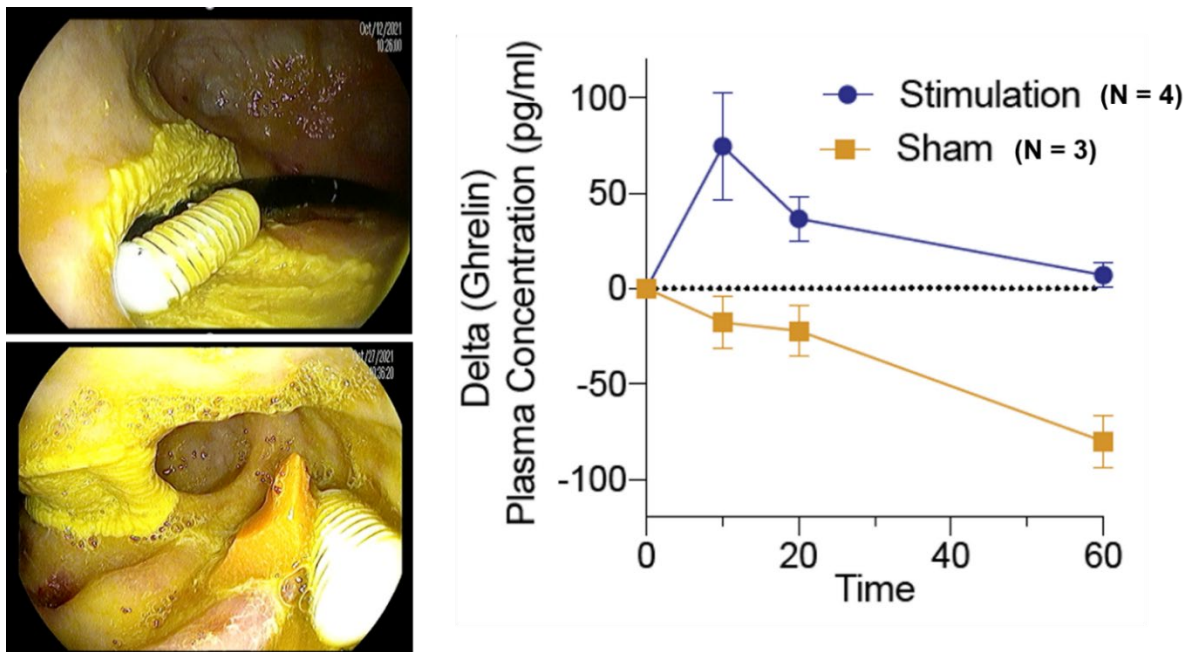


Figure 12. Depiction of Optimized Capsule In Vivo Administration and Plasma Hormone Levels

The same procedure for collecting and analyzing blood as the endoscopic gold probe procedure was performed. These samples were analyzed using a ghrelin ELISA. It was determined that, compared to sham, there was a significant increase in plasma ghrelin after administration of the electrical stimulation capsule at N=4, as shown in Figure 12.

4.2 Device Safety

The next three criteria to be evaluated all focus on the safety of the device via ensuring the ability for localized delivery, safe passage, and no inflammation or scarring in the GI tract.

4.2.1 Localized Deployment

As discussed previously, localized deployment of the capsule system is critical to ensure that the device does not prematurely stimulate the esophagus or upper stomach which would have unintended consequences. Additionally, it prevents premature fluid wicking which could also hinder device functionality. In order to address this concern, a solid capsule shell that could house the capsule, be temporarily sealed, and fall off once administered was developed, as shown in Figure 13. The capsule is placed in the two shell halves and the two halves are sealed using a soldering iron to melt isomalt sugar that will wick into the seam of the two shell halves and solidify, resulting in a temporary water-tight seal.

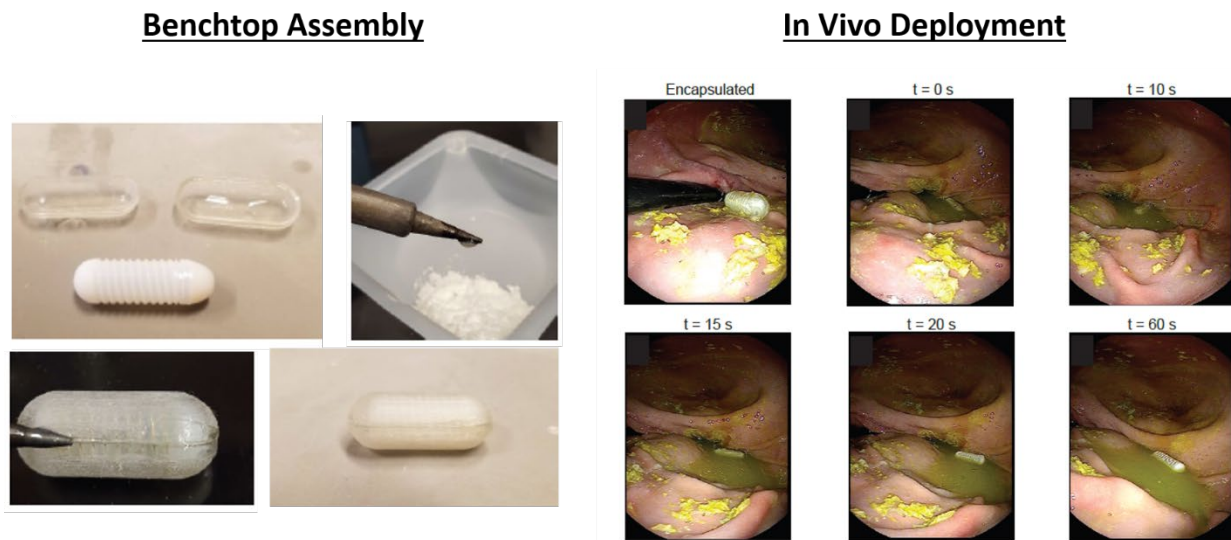


Figure 13. Depiction of Localized Deployment System Assembly and In Vivo Deployment

Once the capsule is administered, the sugar will degrade and eventually release capsule. This demonstration was done in vivo to determine its feasibility, as shown in Figure 13. The encapsulated capsule was administered to the stomach and then subsequently pushed into a small puddle of gastric fluid. Within one minute the capsule shell seal degraded and the shell fell off, deploying the stimulation capsule.

4.2.2 Passage Safety

Next, to determine passage safety six dummy capsules were fabricated and assembled. Three devices were delivered to two pigs each. These devices were tracked via x-ray as they passed the GI tract and were collected after passage, if possible. Figure 14 highlights the workflow for a passage study from validation of administration, tracking via x-ray, and retrieval after excretion. All passage studies were compiled into the violin chart in Figure 14 which shows passage times ranging from 5 days to 14 days, which is fairly typically for devices of this size in pigs.

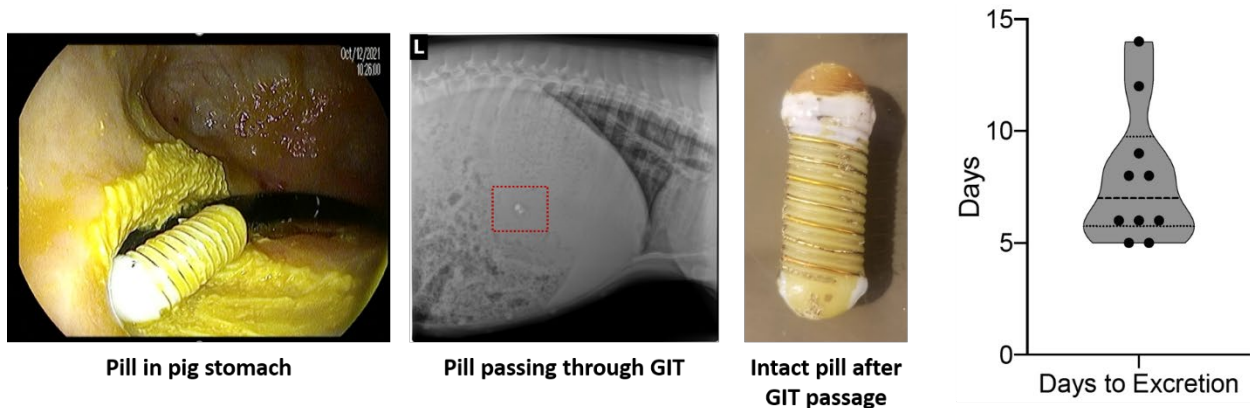


Figure 14. Administration, x-ray evaluation, post-passage collection, and violin distribution chart of passage studies.

Next, the two pigs that were administered 3 pills each were eventually euthanized in a terminal experiment. After the euthanasia, tissue samples were collected from both pigs from the stomach, small intestine (duodenum, jejunum, ileum), and colon (proximal and distal). These samples were then fixed in formalin for 24 hours before transferring to 70% ethanol for long term storage. These were then embedded in paraffin and stained with both H&E and trichrome as shown in Figure 15.

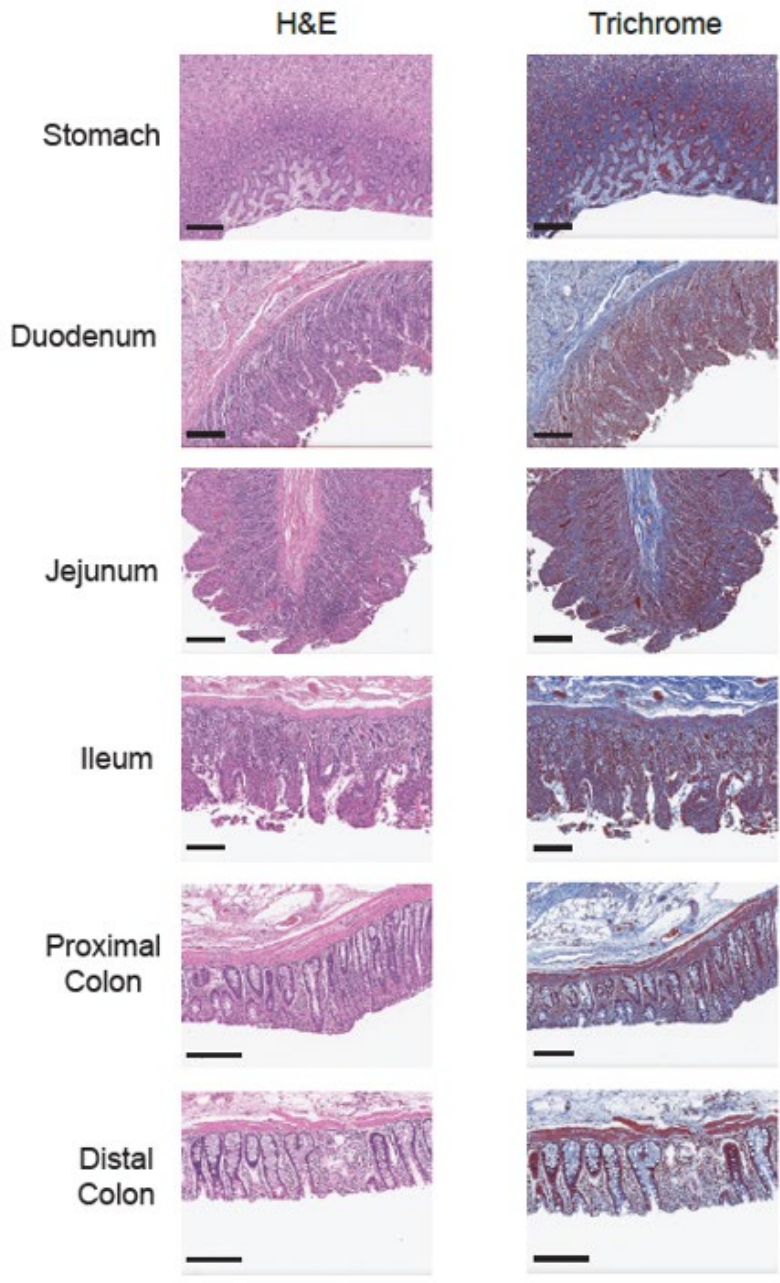


Figure 15. Histology Samples from Various GIT Sections Following Device Passage

These samples were inspected alongside Dr. Bronson of the Koch Institute Histology Core where he determined that there were no signs of inflammation or damage caused to these samples as a result of the administered devices.

5. Conclusion

This body of work as described above demonstrates for the first time a non-invasive ingestible fluid-wicking electrical stimulation capsule for hormone modulation. This interdisciplinary work leverages electronics, mechanical design, materials, biology, and more to develop a proof-of-concept stimulation capsule.

5.1 Discussion

Current commercial GES systems have significant challenges in that they are bulky and require surgical implantation for proper functionality. Given that these systems only reduce the symptoms and do not address the underlying condition, it is a fairly high barrier to overcome for a patient to adopt these systems. This led to the realization that this GES paradigm may be able to be incorporated into a capsule form factor.

Before moving directly to a capsule form factor, *in vivo* (large animal; swine) studies were done to validate that GES performed from inside the stomach on the mucosal surface can induce changes in hormone levels in the blood plasma. During these preliminary studies, the electrical stimulation parameters (pulse width, amplitude, and overall time) were evaluated as well to determine optimal stimulation parameters. It was determined that stimulation parameters of 0.5 mA amplitude, 0.3 ms pulse width at 14 Hz for 20 minutes was sufficient and optimal. These parameters are also similar to those delivered by the commercial Medtronic Enterra™ systems. Additionally, studies were done in pigs that had undergone bilateral vagotomy to better understand potential mechanisms of ghrelin modulation, given that the vagus nerve is the main nerve connection the central nervous system to the enteric nervous system. It was observed that stimulation in vagotomized animals did not show the same ghrelin response as in non-vagotomized animals. In fact, these studies showed a significant decrease in plasma ghrelin levels.

With mucosal GES for hormone modulation validated, the next step was to demonstrate this affect in a capsule form factor. When developing an ingestible capsule that must interact with the gastric mucosa to deliver stimulation, there are two main challenges: 1) contact resistance and 2) managing the gastric environment, especially with respect to gastric fluid that can act as a parasitic loss for the electrical stimulation that should be getting delivered to a specific location in the mucosa. To address these challenges the electrode material must be optimized to reduce contact resistance and the form factor must be optimized to effectively manage the gastric fluid.

Given the broad design space for these ingestible systems, a benchtop testing setup that facilitates rapid prototype evaluation which also mimics the stomach environment is critical to design optimization. To address this, an agarose phantom (2 weight % agarose in PBS) was developed and integrated with electrical characterization systems (oscilloscope, impedance analyzer) to allow for rapid prototype evaluation. The agarose mechanical and electrical properties replicated that of stomach tissue such that the way the capsule interacted with the tissue and how the stimulation propagated in the film were as close to in vivo conditions as possible.

To optimize the electrode materials a range of potential electrodes were evaluated on the agarose setup. This resulted in 14K gold wire being the optimal choice given its resistance to corrosion, relative affordability, and ease of integration compared to alternatives. To optimize form factor, 000 dimensions (9.5x26 mm) informed the volumetric boundary conditions. Additionally, the wire pitch on the external electrodes was minimized. Finally, fluid-wicking grooves that run circumferentially around the capsule were incorporated and optimized in order to serve as fluid wicking channels that can remove gastric fluid from the electrode-mucosa interface. The fluid wicking grooves were optimized by theoretical and experimental approaches. First, they were modeled as vertical capillary channels and were optimized by modulating the groove dimensions and fluid-channel contact angle. This led to the observation that rectangular cross-section grooves at high plasma treatment are optimal. From there, benchtop experiments were conducted to determine the optimal rectangular groove dimensions. There was general agreement on optimal groove dimensions between the experimental and theoretical results.

These optimized grooves were integrated into the capsule system and were then used in in vivo experiments. In vivo demonstrations of these optimized capsules focused around 4 main areas. First, the capsule demonstrated the capability to modulate ghrelin levels in the blood plasma. Second, a temporary external protective shell was developed to ensure localized delivery to prevent premature stimulation and fluid wicking. Third, capsules were administered to pigs and tracked via x-ray and collection after excretion to ensure safe passage. Finally, histology samples were taken from along the GI tract to ensure in a terminal setting to evaluate for any inflammation that may be a result of the device passing through the GI tract and none was observed. All of these in vivo demonstrations indicate to the safety of the device as well as its potential therapeutic benefits.

5.2 Future Work

There are many potential avenues for future work. First, varying the stimulation parameters and location of stimulation may result in different observed biological and physiological effects. Different stimulation parameters may activate different pathways, and different GI tract locations both inside and outside the stomach will play significantly different roles in which stimulation may induce different effects. There is much more space to evaluate and characterize the effects of stimulation in the GI tract. Additionally, more work can be done to better understand the specific mechanisms of stimulation. This work done in vagotomized animals is only the beginning towards answering these questions.

Moving towards the other developments within this project, the paradigm of passive fluid wicking has a multitude of applications. Tailoring the surface properties of ingestible systems to interact differently with the fluidic environment of the stomach is a poorly explored area. Immediate applications could be in serial fluid sampling where hydrophilic channels are used to sample gastric fluid and sense various analytes. The passive nature of the fluid wicking system would allow for significantly higher capability at lower size, weight, and power given that all sampling systems today leverage motorized and electronic parts that have high volume and power budgets. Additionally, the fluid wicking behavior can be utilized for improving mucoadhesive systems given that the hydrophilic nature of the surface results in an attractive capillary force on the device surface. Form factors could be developed that optimize the capillary force with the device weight to ensure proper muco-adhesion in tandem with other chemical adhesion approaches.

Finally, further development can be taken on the GES capsule demonstrated in this work. Immediate next steps could aim to integrate wireless communication so that device status can be monitored, stimulation can be turned on or off depending on its location, and more. Additionally, retention mechanisms can be integrated into these systems so that long-term stimulation can be performed. In this scenario, methods for increasing battery lifetime by energy harvesting or wireless power transfer would likely have to be explored.

Bibliography

- [1] K. Suganya and B.-S. Koo, “Gut–Brain Axis: Role of Gut Microbiota on Neurological Disorders and How Probiotics/Prebiotics Beneficially Modulate Microbial and Immune Pathways to Improve Brain Functions,” *Int. J. Mol. Sci.*, vol. 21, no. 20, Art. no. 20, Jan. 2020, doi: 10.3390/ijms21207551.
- [2] A. Gaman and B. Kuo, “Neuromodulatory Processes of the Brain–Gut Axis,” *Neuromodulation Technol. Neural Interface*, vol. 11, no. 4, Art. no. 4, Nov. 2008, doi: 10.1111/j.1525-1403.2008.00172.x.
- [3] A. E. Bharucha *et al.*, “RELATIONSHIP BETWEEN GLYCEMIC CONTROL AND GASTRIC EMPTYING IN POORLY CONTROLLED TYPE 2 DIABETES,” *Clin. Gastroenterol. Hepatol. Off. Clin. Pract. J. Am. Gastroenterol. Assoc.*, vol. 13, no. 3, pp. 466-476.e1, Mar. 2015, doi: 10.1016/j.cgh.2014.06.034.
- [4] C. D. Vélez and B. Kuo, “Chapter 9 - Gastroparesis and the brain-gut axis,” in *Gastroparesis*, R. W. McCallum and H. P. Parkman, Eds. Academic Press, 2021, pp. 95–107. doi: 10.1016/B978-0-12-818586-5.00009-0.
- [5] K. Nemani, R. Hosseini Ghomi, B. McCormick, and X. Fan, “Schizophrenia and the gut–brain axis,” *Prog. Neuropsychopharmacol. Biol. Psychiatry*, vol. 56, pp. 155–160, Jan. 2015, doi: 10.1016/j.pnpbp.2014.08.018.
- [6] A. I. Petra, S. Panagiotidou, E. Hatzigelaki, J. M. Stewart, P. Conti, and T. C. Theoharides, “Gut-Microbiota-Brain Axis and Its Effect on Neuropsychiatric Disorders With Suspected Immune Dysregulation,” *Clin. Ther.*, vol. 37, no. 5, pp. 984–995, May 2015, doi: 10.1016/j.clinthera.2015.04.002.
- [7] M. Genedi, I. E. Janmaat, B. (Benno) C. M. Haarman, and I. E. C. Sommer, “Dysregulation of the gut–brain axis in schizophrenia and bipolar disorder: probiotic supplementation as a supportive treatment in psychiatric disorders,” *Curr. Opin. Psychiatry*, vol. 32, no. 3, pp. 185–195, May 2019, doi: 10.1097/YCO.0000000000000499.
- [8] G. Kaur *et al.*, “Dysregulation of the Gut-Brain Axis, Dysbiosis and Influence of Numerous Factors on Gut Microbiota Associated Parkinson’s Disease,” *Curr. Neuropharmacol.*, vol. 19, no. 2, pp. 233–247, Feb. 2021, doi: 10.2174/1570159X18666200606233050.
- [9] K. B. Ramadi, S. S. Srinivasan, and G. Traverso, “Electroceuticals in the Gastrointestinal Tract,” *Trends Pharmacol. Sci.*, vol. 41, no. 12, Art. no. 12, Dec. 2020, doi: 10.1016/j.tips.2020.09.014.
- [10] T. L. Abell *et al.*, “Treatment of gastroparesis: a multidisciplinary clinical review,” *Neurogastroenterol. Motil.*, vol. 18, no. 4, pp. 263–283, 2006, doi: 10.1111/j.1365-2982.2006.00760.x.

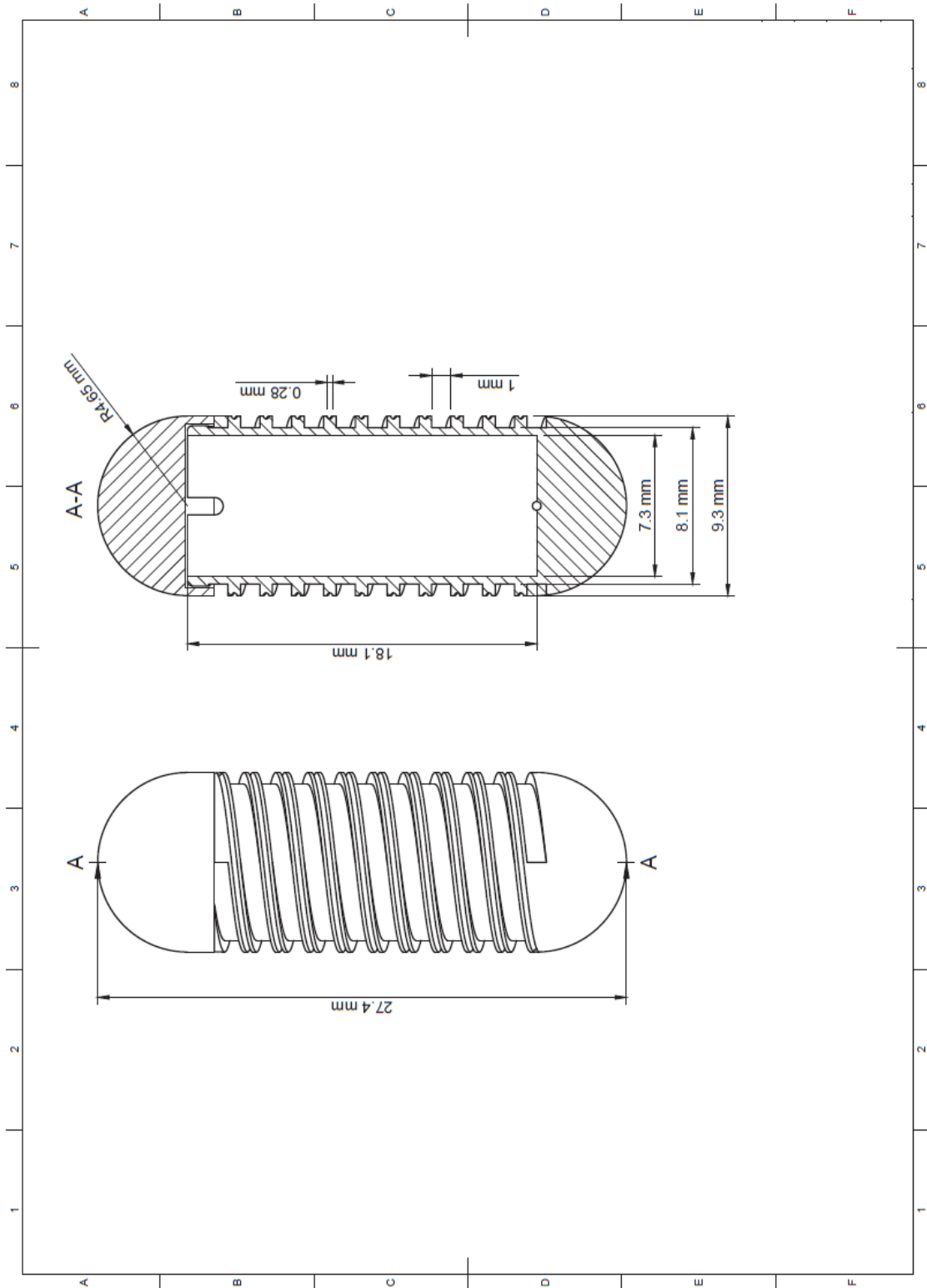
- [11] M. Grover, G. Farrugia, and V. Stanghellini, “Gastroparesis: a turning point in understanding and treatment,” *Gut*, vol. 68, no. 12, pp. 2238–2250, Dec. 2019, doi: 10.1136/gutjnl-2019-318712.
- [12] J. Zhang and J. D. Z. Chen, “Systematic review: applications and future of gastric electrical stimulation,” *Aliment. Pharmacol. Ther.*, vol. 24, no. 7, pp. 991–1002, 2006, doi: 10.1111/j.1365-2036.2006.03087.x.
- [13] T. Abell *et al.*, “Gastric electrical stimulation for medically refractory gastroparesis,” *Gastroenterology*, vol. 125, no. 2, pp. 421–428, Aug. 2003, doi: 10.1016/S0016-5085(03)00878-3.
- [14] W. L. Hasler, “Methods of gastric electrical stimulation and pacing: a review of their benefits and mechanisms of action in gastroparesis and obesity,” *Neurogastroenterol. Motil.*, vol. 21, no. 3, pp. 229–243, 2009, doi: 10.1111/j.1365-2982.2009.01277.x.
- [15] M. Meleine *et al.*, “Gastrointestinal Peptides During Chronic Gastric Electrical Stimulation in Patients With Intractable Vomiting,” *Neuromodulation Technol. Neural Interface*, vol. 20, no. 8, pp. 774–782, Dec. 2017, doi: 10.1111/ner.12645.
- [16] A. Abramson *et al.*, “Ingestible transiently anchoring electronics for microstimulation and conductive signaling,” *Sci. Adv.*, vol. 6, no. 35, p. eaaz0127, Aug. 2020, doi: 10.1126/sciadv.aaz0127.
- [17] S. C. Payne, J. B. Furness, and M. J. Stebbing, “Bioelectric neuromodulation for gastrointestinal disorders: effectiveness and mechanisms,” *Nat. Rev. Gastroenterol. Hepatol.*, vol. 16, no. 2, Art. no. 2, Feb. 2019, doi: 10.1038/s41575-018-0078-6.
- [18] M. P. Jones, C. C. Ebert, and K. Murayama, “Enterra for gastroparesis,” *Am. J. Gastroenterol.*, vol. 98, no. 11, p. 2578, Nov. 2003, doi: 10.1111/j.1572-0241.2003.08681.x.
- [19] H. C. Gonzalez and V. Velanovich, “Enterra® Therapy: gastric neurostimulator for gastroparesis,” *Expert Rev. Med. Devices*, vol. 7, no. 3, pp. 319–332, May 2010, doi: 10.1586/erd.10.4.
- [20] T. L. Abell *et al.*, “Effectiveness of gastric electrical stimulation in gastroparesis: Results from a large prospectively collected database of national gastroparesis registries,” *Neurogastroenterol. Motil.*, vol. 31, no. 12, Art. no. 12, 2019, doi: 10.1111/nmo.13714.
- [21] P. Ducrotte *et al.*, “Gastric Electrical Stimulation Reduces Refractory Vomiting in a Randomized Crossover Trial,” *Gastroenterology*, vol. 158, no. 3, Art. no. 3, Feb. 2020, doi: 10.1053/j.gastro.2019.10.018.
- [22] R. W. McCallum, W. Snape, F. Brody, J. Wo, H. P. Parkman, and T. Nowak, “Gastric Electrical Stimulation With Enterra Therapy Improves Symptoms From Diabetic Gastroparesis in a Prospective Study,” *Clin. Gastroenterol. Hepatol.*, vol. 8, no. 11, pp. 947-954.e1, Nov. 2010, doi: 10.1016/j.cgh.2010.05.020.

- [23] R. W. McCallum, Z. Lin, J. Forster, K. Roeser, Q. Hou, and I. Sarosiek, “Gastric Electrical Stimulation Improves Outcomes of Patients With Gastroparesis for up to 10 Years,” *Clin. Gastroenterol. Hepatol.*, vol. 9, no. 4, pp. 314-319.e1, Apr. 2011, doi: 10.1016/j.cgh.2010.12.013.
- [24] R. W. McCallum *et al.*, “Gastric electrical stimulation with Enterra therapy improves symptoms of idiopathic gastroparesis,” *Neurogastroenterol. Motil.*, vol. 25, no. 10, pp. 815-e636, 2013, doi: 10.1111/nmo.12185.
- [25] S. Gallas *et al.*, “Gastric electrical stimulation increases ghrelin production and inhibits catecholaminergic brainstem neurons in rats,” *Eur. J. Neurosci.*, vol. 33, no. 2, pp. 276–284, Jan. 2011, doi: 10.1111/j.1460-9568.2010.07474.x.
- [26] G. J. Sanger and J. B. Furness, “Ghrelin and motilin receptors as drug targets for gastrointestinal disorders,” *Nat. Rev. Gastroenterol. Hepatol.*, vol. 13, no. 1, Art. no. 1, Jan. 2016, doi: 10.1038/nrgastro.2015.163.
- [27] J. Davis, “Hunger, ghrelin and the gut,” *Brain Res.*, vol. 1693, pp. 154–158, Aug. 2018, doi: 10.1016/j.brainres.2018.01.024.
- [28] ASGE technology committee *et al.*, “Devices for endoscopic hemostasis of nonvariceal GI bleeding (with videos),” *VideoGIE Off. Video J. Am. Soc. Gastrointest. Endosc.*, vol. 4, no. 7, pp. 285–299, Jul. 2019, doi: 10.1016/j.vgie.2019.02.004.
- [29] S. L. Prescott and S. D. Liberles, “Internal senses of the vagus nerve,” *Neuron*, vol. 110, no. 4, pp. 579–599, Feb. 2022, doi: 10.1016/j.neuron.2021.12.020.
- [30] D. M. Bass, M. Prevo, and D. S. Waxman, “Gastrointestinal safety of an extended-release, nondeformable, oral dosage form (OROS: a retrospective study,” *Drug Saf.*, vol. 25, no. 14, pp. 1021–1033, 2002, doi: 10.2165/00002018-200225140-00004.
- [31] M. D. Mitchell, H. L. Kundel, L. Axel, and P. M. Joseph, “Agarose as a tissue equivalent phantom material for NMR imaging,” *Magn. Reson. Imaging*, vol. 4, no. 3, pp. 263–266, Jan. 1986, doi: 10.1016/0730-725X(86)91068-4.
- [32] Z.-J. Chen *et al.*, “A realistic brain tissue phantom for intraparenchymal infusion studies,” *J. Neurosurg.*, vol. 101, no. 2, pp. 314–322, Aug. 2004, doi: 10.3171/jns.2004.101.2.0314.
- [33] J. M. Walker *et al.*, “Nondestructive Evaluation of Hydrogel Mechanical Properties Using Ultrasound,” *Ann. Biomed. Eng.*, vol. 39, no. 10, p. 2521, Jul. 2011, doi: 10.1007/s10439-011-0351-0.
- [34] Y. Lim, D. Deo, T. P. Singh, D. B. Jones, and S. De, “In Situ Measurement and Modeling of Biomechanical Response of Human Cadaveric Soft Tissues for Physics-Based Surgical Simulation,” *Surg. Endosc.*, vol. 23, no. 6, pp. 1298–1307, Jun. 2009, doi: 10.1007/s00464-008-0154-z.

[35] G. Bamorovat Abadi and M. Bahrami, “A general form of capillary rise equation in micro-grooves,” *Sci. Rep.*, vol. 10, no. 1, Art. no. 1, Nov. 2020, doi: 10.1038/s41598-020-76682-2.

Appendices

Device Design Details



Device Assembly Procedure

Prototypes were fabricated and assembled as follows:

1. The capsule shells and caps were fabricated via 3D printing, the electrode wires were ordered off of amazon, the PCB electronics were ordered and populated through Journey Circuits Inc (Schaumburg, IL), and the silver oxide batteries were ordered off of Digi-Key.
2. The capsule shell and cap were placed inside an O₂ plasma cleaner (AutoGlow from Glow Research) within MIT.nano for 5 minutes at 100 W.



Step 2

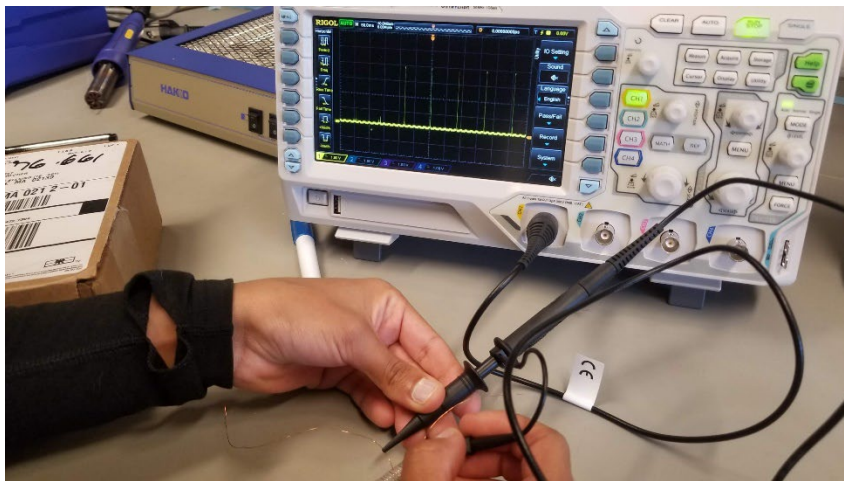
3. Three silver oxide batteries were silver epoxied and/or assembled via Kapton tape in series, and two small pieces of enameled copper wire were attached to the positive and negative terminal of the battery stack with silver epoxy.
4. The gold electrodes were soldered onto the output pads of the PCB.
5. The gold electrode wires were then fed into the capsule and out of the holes on the bottom.

- The battery stack was then soldered onto the input pads of the PCB.



Steps 3-6

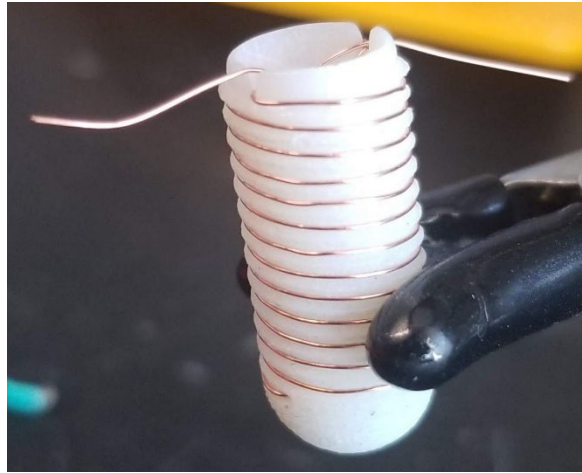
- The entire electronics were tested to ensure that the appropriate pulse profile was being generated before permanently epoxying and assembling the rest of the capsule.



Step 7

- The entire internal electronics assembly was epoxyed together for mechanical robustness and then fed into the capsule where the gold electrodes were pulled out further from the bottom.

9. The electrodes were concentrically wound in their respective grooves and epoxied at the top of the capsule where the cap fits on.



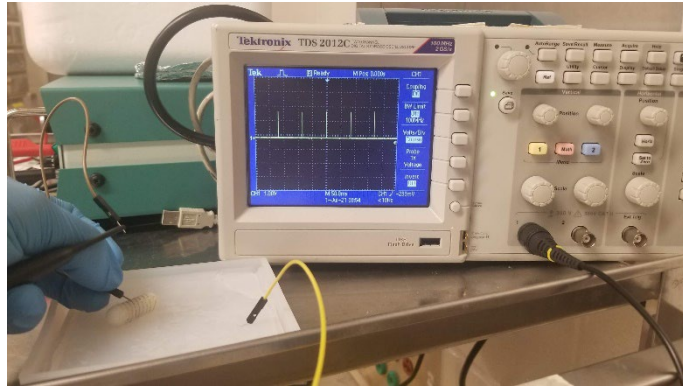
Steps 8-9

10. The cap was then epoxied onto the body and all remaining areas for fluid ingress were epoxied closed.



Step 10

11. The capsule was connected to an oscilloscope through the agarose phantom once to more as a final performance validation before in vivo administration.



Step 11